

An Imidazole Thione-Modified Polyhedral Oligomeric Silsesquioxane for Selective Detection and Adsorptive Recovery of Au(III) from Aqueous Solutions

Zixu Chen, Dengxu Wang,* Shengyu Feng,* and Hongzhi Liu



Cite This: *ACS Appl. Mater. Interfaces* 2021, 13, 23592–23605



Read Online

ACCESS |

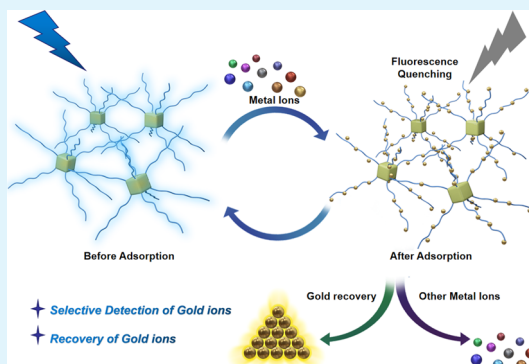
Metrics & More

Article Recommendations

Supporting Information

ABSTRACT: Developing a material toward simultaneous detection and recovery of gold ions (Au(III)) is highly desirable for the economy and the environment. Herein, we report a highly efficient dual-function material for simultaneous Au(III) detection and recovery by simply introducing abundant imidazole thione and thioether groups in one system. This material, that is, an imidazole thione-modified polyhedral oligomeric silsesquioxane (POSS-2), was prepared by a mild reaction of an imidazolium-containing POSS and sulfur at ambient temperature. The POSS-2 suspension in water can rapidly and selectively detect Au(III) with a very low limit of detection of 1.2 ppb by fluorescence quenching or a visualized color change from white to dark orange. POSS-2 can also selectively and efficiently capture Au(III) with a maximum adsorption uptake of 1486.5 mg/g. The adsorption process well fits with the pseudo-second-order kinetic and Langmuir models. The intriguing dual-function performance is better than most of the previous Au(III) probes or adsorbents. The mechanism study reveals that the detection and adsorption behavior are mainly caused by the redox reaction and coordination between imidazole thione and thioether groups and Au(III). Furthermore, POSS-2 was successfully utilized to extract gold without interference from a discard CPU. These results indicate the potential application of the present dual-function material for Au(III) detection and recovery from aqueous solutions. More dual-functional materials could be designed and prepared by this simple strategy.

KEYWORDS: silsesquioxane, gold recovery, gold detection, electronic wastes, imidazole thione



INTRODUCTION

Gold as an ancient precious metal is widely used in many areas, especially in high-tech electronics, such as printed boards, diodes, and connectors, due to its excellent electrical conductivity, good ductility, and outstanding inherent inertness for corrosion resistance.¹ Unfortunately, with the rapid development of industry, a mass of gold-containing wastewater and electronic wastes is generated and has posed a serious threat to the environment and human beings. For instance, the binding of gold ions (Au(III)) with DNA or enzymes has negative effects on the kidney, liver, and even the whole nervous system of human beings.² Gold from industrial sewage will be enriched in plants and animals. However, a low content of gold ions, especially <10 ppb in water, is difficult to detect.³ Meanwhile, the limited and decreased natural gold ores and the growing demand for gold have prompted an urgent requirement for recovering gold species from Au-containing wastes and wastewaters. As a result of these attributes, developing an efficient and environmentally friendly method for Au(III) detection and recovery is significant because of great importance for environment protection and full utilization of Au-containing secondary resources.

Due to the high cost, complexity, and time consumption in conventional methods, fluorescence detection has become the most widespread method for Au(III) detection due to its high sensitivity and facile operation.^{4,5} Many Au(III) fluorescent probes with limits of detection (LOD) as low as ppb level have been designed and developed from the reaction or coordination sensing mechanism.^{6–8} From the viewpoint of Au(III) recovery, adsorptive capture is the most common method due to its low cost, simplicity, and high efficiency. Numerous Au(III) adsorbents have been presented with a maximum adsorption capacity of up to 3257.3 mg/g.^{9–11} However, most reports focus on one aspect, that is, detection or recovery of Au(III). Few of them have aimed at the materials involving simultaneous detection by fluorometry and

Received: January 29, 2021

Accepted: May 4, 2021

Published: May 13, 2021



recovery by adsorption of Au(III), probably because it is difficult to balance these two functions.^{12–14} In other words, it is difficult to efficiently recover Au(III) in Au(III) probes with high detection efficiencies due to the lack of adsorbable functional groups, or Au(III) adsorbents with high recovery efficiencies are not suitable for detection due to the lack of fluorescence sensitivity. Developing dual-function materials toward simultaneous Au(III) detection and recovery with high sensitivity, selectivity, and recovery efficiency is still highly desirable.

To realize this goal, the dual-function material can be designed on the basis of two principles. First, it should be designed to possess specific functional groups, which can interact with Au(III) to trigger the fluorescence “turn-on” or “turn-off” or color change (named the colorimetric assay) and thus achieve the detection of Au(III).⁴ Second, it is necessary to introduce abundant functional units (e.g., persimmon tannin,¹⁵ chitosan,¹⁶ thiourea,⁹ and sulfur-rich^{6,7}), which can efficiently interact with Au(III) by coordination or a reaction to afford high Au(III) recovery efficiency. More importantly, the selected functional groups are exclusive and can merely interact with Au(III) in the presence of other interfering metal ions, thereby leading to selective detection and recovery.

Combining these attributes, herein, we present a dual-function material toward Au(III) detection and recovery, that is, octa(1-methyl-3-(3-propylsulfanyl-propyl)-1,3-dihydro-imidazole-2-thione)silsesquioxane (POSS-2). The introduction of imidazole thione groups imparts the material with high fluorescence, which can be utilized to selectively detect Au(III) by fluorescence quenching. The idea “inorganic–organic” and bulky polyhedral oligomeric silsesquioxane (POSS) unit can enhance thermal stability and suppress the aggregation to alleviate fluorescence quenching in the solid state.¹⁸ This feature is beneficial to fluorescence detection. The abundant imidazole thione and thioether groups within POSS-2 enable it to have a high recovery ability toward Au(III) by coordination interaction and redox reaction of Au(III) to zero-valent gold (Au(0)). In addition, the hydrophobic Si–O–Si units in POSS can facilitate the separation and reusability of the material in the aqueous-phase application process. With our expectation, POSS-2 exhibits high sensitivity and selectivity toward Au(III) with a limit of detection of 1.2 ppb, as well as high selectivity and an adsorption capacity of 1486.5 mg/g, indicating its promising potential for selectively detecting and recovering Au(III) from aqueous solutions.

EXPERIMENTAL SECTION

Materials. Commercially available reagents were purchased from Energy Chemical and used without purification. 1-Methyl-3-(2-propen-1-yl)imidazolium bromide (M-1)¹⁹ and octamercaptopropyl-silsesquioxane (POSS-SH)²⁰ were prepared by previous methods.

Synthesis of Octa(1-methyl-3-(3-propylsulfanyl-propyl)-imidazolium bromide)silsesquioxane (POSS-1). In a flask, POSS-SH (1.0 g, 0.98 mmol), M-1 (1.6 g, 7.9 mmol), and 2,2-dimethoxy-2-phenylacetophenone (DMPA) (0.05 g) were dissolved in a mixed solvent of CH₂Cl₂ and CH₃OH (volume ratio of 1:1, 15 mL). Then, the mixture was irradiated by a UV lamp for 30 min and the solvents were removed under vacuum. The resultant oil was washed with CH₂Cl₂ several times to remove the unreacted reactants and DMPA and dried overnight. The final product POSS-1 was afforded as a yellow viscous oil (2.43 g, 93.6%). IR (KBr pellet cm⁻¹): 3140, 3066, 2928, 2862, 1620, 1572, 1452, 1344, 1292, 1254, 1099, 818, 758, 706, 619, 544, 480. ¹H NMR (CD₃OD, 400 MHz): δ 9.09 (s, 8H), 7.70 (s, 8H), 7.59 (s, 8H), 4.37 (s, 16H), 3.95 (s, 24H), 2.56 (s, 32H), 2.17 (d, 16H), 1.67 (s, 16H), 0.76 (s, 16H); ¹³C NMR

(CD₃OD, 125 MHz): δ 136.74, 124.26, 122.45, 36.50, 33.88, 29.57, 28.17, 22.83, 10.60; ²⁹Si NMR (CD₃OD, 75 MHz): δ -66.68. Elemental analysis calcd (%) for C₈₀H₁₄₄Br₈N₁₆S₈Si₈O₁₂: C 36.36, H 5.45, N 8.48, S 9.71; found: C 36.40, H 5.41, N 8.43, S 9.65.

Synthesis of Octa(1-methyl-3-(3-propylsulfanyl-propyl)-1,3-dihydro-imidazole-2-thione)silsesquioxane (POSS-2). POSS-1 (1.321 g, 0.5 mmol), K₂CO₃ (1.105 g, 8 mmol), sulfur powder (0.256 g, 8 mmol), and methanol (10 mL) were placed in a flask under constant stirring at reflux temperature (65 °C) for 24 h. The crude product was obtained after filtration and evaporation of the solvent. The residue was extracted with CHCl₃ (20 mL) and filtered to remove the impurities. The filtrate was rotary evaporated, affording the crude product. After washing the crude product with 10 mL of methanol three times and subsequent drying in vacuo at 60 °C for 6 h, a light yellow solid was obtained as the final product (0.811 g, yield: 72%). IR (KBr pellet cm⁻¹): 3118, 2928, 1677, 1564, 1455, 1407, 1338, 1237, 1127, 1033, 798, 712, 673, 528, 471. ¹H NMR (400 MHz, CDCl₃) δ 6.71 (d, 16H), 3.99 (s, 16H), 3.45 (s, 24H), 2.43 (s, 32H), 1.95 (d, 16H), 1.64 (s, 16H), 0.59 (s, 16H). ¹³C NMR (100 MHz, CDCl₃): δ 159.83, 116.96, 116.24, 19.5, 45.37, 33.72, 27.55, 22.23, 11.55. ²⁹Si NMR (75 MHz, CDCl₃): δ -67.07. Elemental analysis calcd (%) for C₈₀H₁₃₆N₁₆S₁₆Si₈O₁₂: C 42.67, H 6.09, N 9.95, S 22.78; found: C 42.65, H 6.08, N 9.78, S 22.19.

Detection of Au(III) Ions by POSS-2 in Aqueous Solutions. A typical procedure was described as follows. A POSS-2 suspension (0.1 mg/mL) was first prepared by adding dried POSS-2 (3 mg) into deionized water (30 mL) and dispersed uniformly by ultrasonication. To evaluate the detection of Au(III) by POSS-2, successive concentrations of AuCl₃·HCl·4H₂O (0–100 ppm) in aqueous solutions were added into the POSS-2 suspensions and their fluorescence spectra were recorded by a fluorescence spectrophotometer.

Selective Detection of Au(III). First, the fluorescence emission spectra of POSS-2 suspensions (0.1 mg/mL) in the presence of various metal ions, including K(I), Na(I), Ca(II), Mg(II), Al(III), Zn(II), Ni(II), Pb(II), Cd(II), Cr(III), and Mn(II) ions, in aqueous solutions (100 ppm) were measured. Then, to evaluate the detection selectivity, the fluorescent spectra of POSS-2 suspensions (0.1 mg/mL) in the coexistence of equivalent Au(III) and competing metal ions (100 ppm) were recorded.

Effect of pH. The effect of pH on the detection efficiency was investigated by adjusting the pH of the mixture containing Au(III) (50 ppm) and POSS-2 suspension (0.1 mg/mL) in the pH range from 1 to 7. Hydrochloric acid and sodium hydroxide were used to adjust the pH.

Calculating the Limit of Detection (LOD). The limit of detection (LOD) for Au(III) was calculated using eq 1 as follows

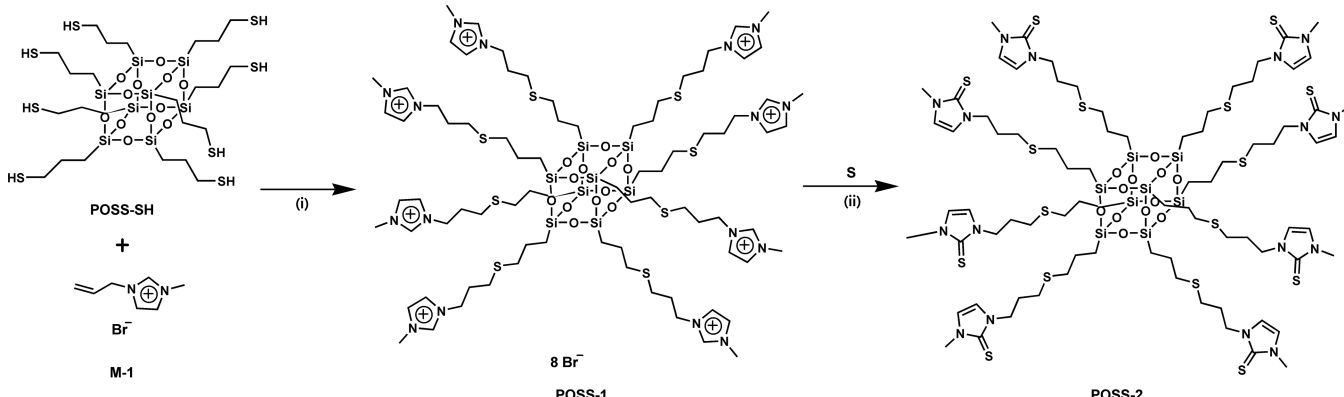
$$\text{LOD} = 3 \times \sigma/K \quad (1)$$

where σ represents the standard deviation of blank measurement, which was obtained by recording the fluorescence intensity of the POSS-2 suspension in aqueous solution six times. The parameter K is the slope of fluorescence emission intensity excited at 270 nm versus the concentration of Au(III) ions.

Analysis of Au(III) Ions in Real Samples. POSS-2 suspensions (0.1 mg/mL) in real water samples were prepared by adding POSS-2 into tap water, well water, and spring water of Black Tiger Spring and dispersed uniformly with an ultrasonic dispersion instrument. Upon addition of two known concentrations (2 and 20 ppm) of Au(III) ions in the POSS-2 suspensions, the fluorescence response of POSS-2 toward Au(III) ions was recorded by a fluorescence spectrophotometer excited at 270 nm.

Adsorption of Au(III) Ions by POSS-2 in Aqueous Solutions. The adsorption of Au(III) (AuCl₃·HCl·4H₂O) by POSS-2 suspensions in water (1 mg/mL) was carried out at room temperature. After the adsorption equilibrium, the resulting solutions were collected by filtration to remove the adsorbents and the Au(III) concentrations were measured by AAS or ICP-MS.

The effect of initial Au(III) concentrations on the adsorption capacity was investigated by adding a series of concentrations,

Scheme 1. Synthetic Route of POSS-2^a

^aReaction conditions: (i) UV, DMPA, CH₂Cl₂/CH₃OH, 30 min; (ii) K₂CO₃, CH₃OH, reflux, 24 h.

including 100, 200, 500, 700, 1000, 2000, 3000, 4000, and 5000 ppm, to the POSS-2 suspensions (1 mg/mL) at 24 h equilibrium.

The effect of contact time on the adsorption capacity was studied by stirring the mixtures comprising Au(III) (2000 ppm) and POSS-2 (1 mg/mL) in aqueous solutions. The concentrations of Au(III) were measured at 5 min, 10 min, 30 min, 1 h, 2 h, 3 h, 4 h, 5 h, 12 h, 24 h, 36 h, and 48 h.

The removal efficiency of Au(III) was evaluated by applying POSS-2 suspensions (1 mg/mL) to remove Au(III) in aqueous solutions with concentrations ranging from 50 to 5000 ppm. The effect of the coexistence of competitive metal ions on the removal efficiency of Au(III) was further assessed by applying POSS-2 suspensions (1 mg/mL) to capture Au(III) (100 ppm) in the presence of one of the interfering metal ions, including Na(I), K(I), Ca(II), Mg(II), Al(III), Cu(II), Fe(III), Ni(II), Pb(II), Cd(II), Cr(III), and Mn(II) ions, at a concentration of 100 ppm under stirring for 1 h.

The effect of pH on the adsorption ability was studied by altering the pH of the mixture comprising Au(III) at three concentrations (100, 1000, and 2000 ppm) and POSS-2 suspension (1 mg/mL) over a pH range of 1–7. The pH was altered by adding HCl and NaOH into the chloroauric acid solution.

The removal efficiency (q (%)) and adsorption capacity (Q_e (mg/g)) were calculated using eqs 2 and 3, respectively

$$q = \frac{C_0 - C_e}{C_0} \times 100 \quad (2)$$

$$Q_e = \frac{C_0 - C_e}{m} \times V \quad (3)$$

where C_0 and C_e (mg/L) are the initial and residual concentrations of Au(III) ions in aqueous solutions, respectively. m (mg) is the mass of POSS-2, and V (L) is the solution volume.

Chi-square statistic (X^2) was calculated to measure the fitness of adsorption results of the isotherm and kinetic models as shown in eq 4^{21,22}

$$X^2 = \frac{100}{n} \sum_i^n \frac{(Q_{e,cal} - Q_{e,exp})^2}{Q_{e,exp}} \quad (4)$$

where n is the number of data points and $Q_{e,cal}$ and $Q_{e,exp}$ are the calculated and experimental adsorption amounts of Au(III) (mg/g), respectively.

Adsorption Equilibrium and Kinetics. The adsorption kinetics was studied by collecting the concentrations of gold ions (2000 ppm) from 5 to 2880 min. The kinetic models, including the pseudo-first-order, pseudo-second-order, and intraparticle diffusion kinetic models, which are expressed as eqs 5, 6, and 7, were applied to fit the experimental results, respectively.

$$\ln(Q_e - Q_t) = \ln Q_e - K_f t \quad (5)$$

$$\frac{t}{Q_t} = \frac{t}{Q_e} + \frac{1}{K_2 Q_e^2} \quad (6)$$

$$Q_t = K_f t^{1/2} + C \quad (7)$$

Q_t (mg/g) and Q_e (mg/g) refer to the adsorption capacity of gold ions at time t and at equilibrium time, respectively. K_1 and K_2 (g/mg·min) are the rate constants of the pseudo-first-order model and pseudo-second-order model, respectively. In addition, K_i (mg/g·min^{1/2}) is related to the rate constant of the intraparticle diffusion model. C is the constant indicative of the boundary layer thickness.

The isotherms of gold ion adsorption were measured at the initial concentrations of Au (III) from 100 to 5000 ppm. Langmuir, Freundlich, and Temkin isotherms were used as adsorption isotherm models, which are expressed as eqs 8, 9, and 10

$$\frac{C_e}{Q_e} = \frac{C_e}{Q_m} + \frac{1}{K_L \times Q_m} \quad (8)$$

$$\ln Q_e = \ln K_F + \frac{1}{n} \times \ln C_e \quad (9)$$

$$Q_e = \left(\frac{R \times T}{b} \right) \times \ln C_e - \frac{R \times T \times \ln K_T}{b} \quad (10)$$

where Q_m (mg/g) and C_e (mg/L) are the maximum adsorption capacity and Au(III) ion concentration at equilibrium, respectively. K_L , K_F , and K_T are the constants related to Langmuir, Freundlich, and Temkin isotherms, respectively, and n is the heterogeneity factor. b refers to the constant, while T and R represent the temperature (K) and gas constant (8.314 J/mol·K), respectively.

Reusability of POSS-2 for Adsorbing Au(III). The adsorption process was conducted by stirring a mixture of POSS-2 (1 mg/mL) and 500 ppm of Au(III) in aqueous solution for 2 h. The mixture was centrifuged to remove the supernatant. The obtained precipitate was washed with deionized water (10 mL) and centrifuged again. Then, the desorption process was carried out by adding ascorbic acid (0.05 M in aqueous solution) in the POSS-2 + Au(III) system for 5 h. After desorption, the mixture was centrifuged to retain the precipitate and washed with 10 mL of deionized water three times. The recycling experiment was repeated five times, and the concentrations of Au(III) in the filtrates were analyzed by AAS.

Gold Recovery by POSS-2 from Electronic Waste. A discarded CPU was obtained from Intel Corporation, and 0.25 g of metal scraps was scratched from the surface of the CPU. SEM-EDX results confirmed that the scraps contain Cu, Ni, and Au elements. Au(III) was then leached from the resulting metal powder by soaking the scraps in a solution containing distilled water (119 mL), pyridine (0.97 mL, 12.0 mmol), and *N*-bromosuccinimide (NBS) (0.75 g, 4.2 mmol) for 24 h.²³ A blue solution was obtained by filtration and acidified for the subsequent elemental analysis. The initial metal

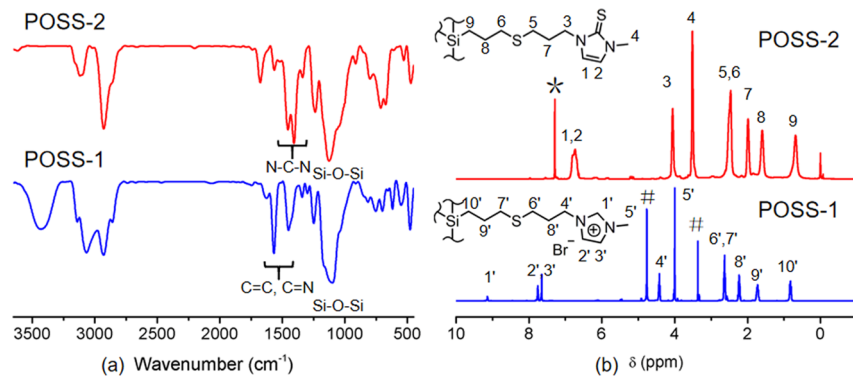


Figure 1. FT-IR spectroscopy (a) and ^1H NMR (b) spectra of POSS-1 and POSS-2. The asterisk and pound denote CDCl_3 and CD_3OD , respectively.

concentrations of Cu(II), Ni(II), and Au(III) were determined by AAS. After the POSS-2 suspension (0.1 mg/mL) was added to the solution, the mixture was stirred for 10 min, 30 min, 1 h, and 2 h. Then, the mixtures were centrifuged and the solutions were collected through a filter membrane with an aperture diameter of $0.22\ \mu\text{m}$. The resultant solutions were measured by AAS to obtain the concentrations of Cu(II), Ni(II), and Au(III).

Gold Recovery by Pyrolysis. POSS-2 (60 mg) was added into Au(III) aqueous solution (40 mL, 2000 ppm), and the resultant mixture was stirred for 24 h. The precipitate was collected by centrifugation for 20 min. The collected precipitate was dried at 40°C in vacuo overnight. The solid was then heated in a furnace under an air atmosphere at 1000°C for 3 h with a heating rate of $10^\circ\text{C}/\text{min}$.²⁴ After treating the solid with hydrofluoric acid for 24 h, a yellow solid with a metallic luster was afforded. The gold content in the sample was measured by AAS.

RESULTS AND DISCUSSION

Synthesis and Characterization. The synthetic route of POSS-2 is shown in Scheme 1. Octa(1-methyl-3-(3-propylsulfanyl-propyl)-imidazolium bromide)silsesquioxane (POSS-1) was first prepared by a thiol-ene reaction of octamercaptotripropylsilsesquioxane (POSS-SH) with 1-methyl-3-(2-propen-1-yl)imidazolium bromide (M-1). Then, POSS-1 reacted with sulfur in the presence of K_2CO_3 at reflux temperature (65°C) for 24 h, yielding the final product octa(1-methyl-3-(3-propylsulfanyl-propyl)-1,3-dihydro-imidazole-2-thione)-silsesquioxane (POSS-2) as a light yellow solid. POSS-2 is soluble in various organic solvents, such as dichloromethane, chloroform, and *N,N*-dimethylformamide, but insoluble in water and methanol. However, it can be well-dispersed in water and this feature is helpful to its applications in aqueous solutions.

POSS-1 and POSS-2 were fully characterized by FT-IR, ^1H NMR, ^{13}C NMR, ^{29}Si NMR, and elemental analysis. In the IR spectra (Figure 1a), the peaks from 1596 to $1433\ \text{cm}^{-1}$ are attributable to the $\text{C}=\text{N}$ or $\text{C}=\text{C}$ stretching vibrations from imidazolium groups in POSS-1. The peak at $1455\ \text{cm}^{-1}$ corresponds to the $\text{N}-\text{C}-\text{N}$ group in the POSS-2 spectrum. The intense peaks at $\sim 1100\ \text{cm}^{-1}$ are apparently attributed to the $\text{Si}-\text{O}-\text{Si}$ stretching vibration. Figure 1b shows the ^1H NMR comparison between POSS-1 and POSS-2. The imidazolium hydrogens ($-\text{N}=\text{CH}-\text{N}-$) in POSS-1 are found at $9.09\ \text{ppm}$, and this peak disappears in POSS-2, indicating the successful formation of imidazole thione. This finding can be also verified by the ^{13}C NMR spectra (Figure S1) in which the peak assigned to the imidazolium carbons ($-\text{N}=\text{CH}-\text{N}-$) in POSS-1 is observed at $136.7\ \text{ppm}$ and a new

peak assigned to the formed $\text{C}=\text{S}$ is observed at $159.8\ \text{ppm}$. As expected, two single peaks are observed at -66.7 and $-67.1\ \text{ppm}$ for POSS-1 and POSS-2, respectively, in the ^{29}Si NMR spectra (Figure S2). The elemental analysis also confirmed the successful achievement of POSS-1 and POSS-2, as evidenced by the accordance between the found and calculated nitrogen and/or sulfur contents of these two compounds. In addition, thermal gravimetric analysis (TGA) reveals that POSS-2 exhibits good thermal stability with a $T_{d,5\%}$ (5% mass loss) of ca. 310°C (Figure S3).

Detection of Au(III) by POSS-2. To evaluate the ability of POSS-2 to detect Au(III), the absorption and fluorescence spectra of the POSS-2 suspension (0.1 mg/mL) and the mixture of Au(III) (100 ppm) and POSS-2 (0.1 mg/mL) were investigated in an aqueous suspension. As shown in Figure 2,

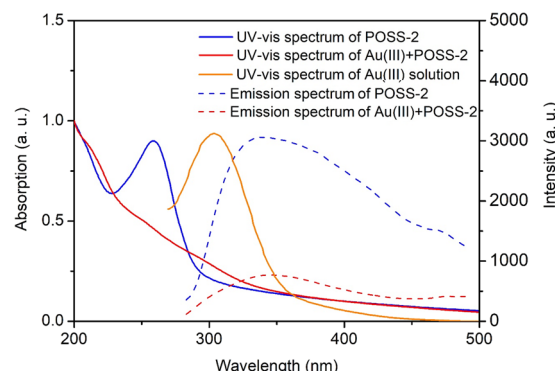


Figure 2. UV-vis absorption of Au(III) in aqueous solution and UV-vis absorption and fluorescence emission spectra of the POSS-2 suspension in water (0.1 mg/mL) and POSS-2 suspension (0.1 mg/mL) in the presence of Au(III) (100 ppm) ($\lambda_{\text{ex}} = 260\ \text{nm}$).

POSS-2 exhibits a narrow absorption band in the range of 200 – $300\ \text{nm}$ with the maximum absorption peak at $260\ \text{nm}$ and strong fluorescence at 300 – $500\ \text{nm}$ excited at $260\ \text{nm}$. This finding can be attributed to the $n-\pi^*$ transitions of imidazole thione groups. Upon addition of Au(III), a significant decrement of the absorbance and fluorescence intensities of POSS-2 was observed.

Further, a detection experiment for Au(III) was performed by adding successive concentrations of Au(III) (0–100 ppm) to POSS-2 suspensions in water (0.1 mg/mL). As shown in Figure 3a, the colors of suspensions gradually turned from colorless to reddish orange with a concentration increment of Au(III), allowing the “bare-eye” detection by this probe. It is

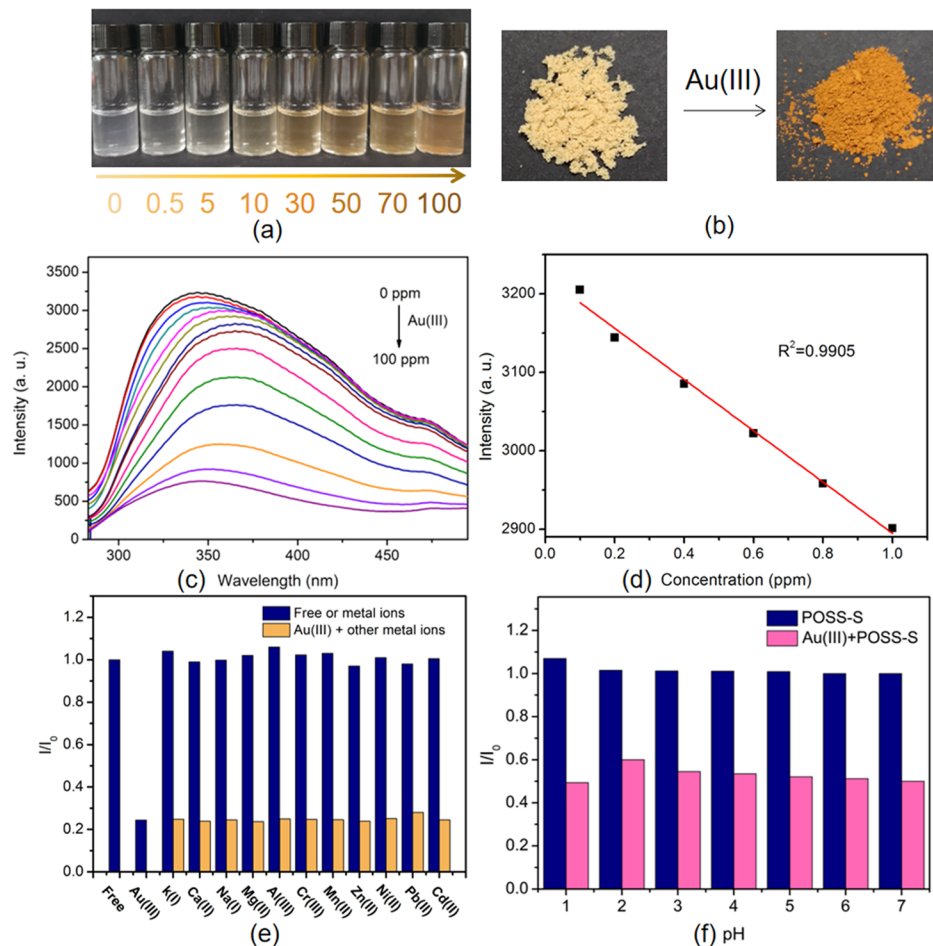


Figure 3. (a) Photograph of POSS-2 suspensions in water (0.1 mg/mL) with the concentrations of Au(III) from 0 to 100 ppm, (b) the photographs of POSS-2 before and after the detection of Au(III), (c) fluorescence quenching spectra of POSS-2 suspensions in water (0.1 mg/mL) with the concentrations of Au(III) from 0 to 100 ppm ($\lambda_{\text{ex}} = 260 \text{ nm}$), (d) the limit of detection calculated by the linear relationship between the emission intensity of the POSS-2 suspension (0.1 mg/mL) and the concentrations of Au(III) from 0 to 1 ppm ($\sigma = 1.36$), and (e) detection selectivity of the POSS-2 suspension toward Au(III) among various metal ions, blue bars represent POSS-2 suspensions with or without one metal ion (100 ppm). Yellow bars represent the subsequent addition of Au(III) (100 ppm) to the suspensions. (f) The effect of pH on the I/I_0 of POSS-2 and POSS-2 with a Au(III) concentration of 50 ppm. Blue bars and pink bars represent POSS-2 suspensions in the absence and presence of Au(III).

Table 1. Detection Comparison of POSS-2 toward Au(III) with Other Sensors

no.	sensors	methods	LOD	detection media	ref
1	nitrogen-doped CDs	flu “turn off”	53 nM	water	2
2	silicon quantum dots	flu “turn off”	13.67 ppb	water	12
3	GO-PVA	flu “turn off”	275 ppb	water	28
4	PEGylated gold nanoparticles	colorimetric, flu “turn off”	25 ppb	water	29
5	bistriazole-bearing boron	flu “turn on”	2 μM	MeCN/H ₂ O	30
6	rhodamine-BODIPY	flu “turn on”	65 nM	CH ₃ CN/HEPES	31
7	triazole-linked C-glycosyl pyrene	flu “turn off”	0.14 μM	water	25
8	thiocarbonate-functionalized 2-(2-hydroxyphenyl)benzo thiazole	flu “turn on”	48 nM	water/DMSO	26
9	BODIPY-based fluorescent probe	flu “turn on”	100 nM	water	6
10	conjugate adsorbent	colorimetric	0.11 ppb	water	27
11	POSS-2	colorimetric, flu “turn off”	1.2 ppb (6.1 nM)	water	this work

worthy to note that the color change of suspensions can be visually observed at 10 ppm Au(III). The color transition can be also found in the solid state. The treatment of POSS-2 with Au(III) resulted in a red-orange solid (Figure 3b). The fluorescence titration experiment of POSS-2 was further performed to investigate the quenching behavior of POSS-2 toward Au(III). With an increment of Au(III), the

fluorescence intensity continuously decreased and reached nearly constant at a concentration of 100 ppm (Figure 3c), indicating a “turn-off” fluorescence detection. On the basis of the titration experiment, the limit of detection (LOD) was calculated from the slope of the emission intensity versus the concentration of Au(III) ions (Figure 3d). POSS-2 exhibits a high sensitivity for Au(III) determination with a low LOD of

1.2 ppb (6.1 nM). The value is comparable to or higher than many gold sensors, such as fluorescent silicon quantum dots (13.67 ppb),¹² triazole-linked C-glycosyl pyrene (27.57 ppb),²⁵ thiocarbonate-functionalized 2-(2-hydroxyphenyl) benzothiazole (9.5 ppb),²⁶ and conjugated adsorbent (0.11 ppb).²⁷ The comparison results are summarized in Table 1. The lower performance of the present sensor than some previous sensors may be due to the heterogeneous detection, in contrast to the homogeneous detection of most sensors.

The selective detection of Au(III) among various metal ions is another important factor for the Au(III) sensors. Thus, two control experiments were carried out to evaluate the selectivity. First, various metal ions, including K(I), Na(I), Ca(II), Mg(II), Al(III), Zn(II), Ni(II), Pb(II), Cd(II), Cr(III), Mn(II), and Au(III) ions (100 ppm), were added into the POSS-2 suspensions, and the fluorescence intensities of resultant mixtures were recorded and calculated as I/I_0 (blue bars in Figure 3e). It was found that the fluorescence intensity barely changed after adding other metal ions except Au(III). Subsequently, a competitive experiment was performed by adding the mixture of 100 ppm Au(III) and 100 ppm of interfering metal ions into POSS-2 suspensions. There was no noticeable interference effect after adding the competitive metal ions (yellow bars in Figure 3e), indicating the good selectivity and anti-interference ability of POSS-2.

Moreover, this detection process is very fast. Upon addition of Au(III), a significant reduction of fluorescence intensity was observed within 10 s and stable within 30 s (Figure S4). Additionally, the pH barely influenced the detection efficiency over the pH range of 1–7 as evidenced by the negligible effect on the fluorescence intensity (Figure 3f). These findings clearly reveal that the detection of Au(III) is very rapid and stable, thereby indicating that POSS-2 could serve as a promising sensor for fast and selective detection of Au(III) without strict time control.

The application potential of the present method was also evaluated by applying POSS-2 to detect Au(III) in real environmental water samples, including tap water, well water, and spring water of Black Tiger Spring. The experiments were carried out by adding known concentrations of Au(III) ions (2 and 20 ppm) into POSS-2 suspensions in different water samples, and their fluorescence emission intensities were recorded. As shown in Table S1, the emission intensities were analyzed by the K_{SV} curve (Figure S5) and the obtained values were in good agreement with the actual added concentrations of gold ions (recovery >90%). These results suggest that POSS-2 can be used as a fluorescent probe for sensing Au(III) in real samples.

The quenching phenomenon can be explained by two mechanisms. One is the strong interaction between the thione and thioether ligands and the gold ions, leading to the irreversible formation of a new stable, nonemissive molecular entity.³² The coordination interactions between gold cations and thioethers have been proven in many reports.^{14,33–35} For the imidazole thione unit, due to its intrinsic zwitterionic resonant structure, the sulfur anions and cationic imidazole ring are formed by charge delocalization.³⁶ Then, a coordination complex was also formed by the coordination between Au(III) and sulfur anions in imidazole thione groups.^{37–41} In addition, the charge delocalization can enhance the interactions between the material and AuCl_4^- via electrostatic interaction and thus improve the detection efficiency. The electrostatic interaction can be verified by

zeta potential. The zeta potential of POSS-2 is -4.55 mV and turns to $+17.87\text{ mV}$ after the adsorption of Au(III), indicating the existence of the electrostatic interaction between Au(III) and POSS-2. This mechanism can also well explain the detection selectivity of Au(III) because of the nonformation of the coordination complex with other metal cations. The other mechanism is the fluorescence resonance energy transfer (FRET) from imidazole thione groups in POSS-2 to Au(III), as evidenced by the overlapping absorption band of Au(III) with the emission of POSS-2 (Figure 2).^{42,43} Therefore, the sensitive and selective detection of Au(III) with a low limit is a result of coordinative interactions between sulfur atoms and gold ions and FRET.

Adsorption of Au(III) by POSS-2. Developing an efficient adsorbent for simultaneous detection and removal of Au(III) is highly desirable. As POSS-2 contains abundant sulfur and nitrogen atoms and possesses an excellent sensing performance toward Au(III), it is expected that it has the ability to capture Au(III) from aqueous solutions. To achieve valuable insights into the recovery capacity of POSS-2 for Au(III), the adsorption kinetics was investigated to understand the affinity of POSS-2 toward Au(III). Three conventional kinetic models, including pseudo-first-order, pseudo-second-order, and intraparticle diffusion models, were introduced to fit the experiment results. The kinetic experiments for Au(III) onto POSS-2 were performed from 5 min to 48 h at a Au(III) concentration of 2000 ppm, and the corresponding parameters including correlation coefficients (R^2), kinetic parameters (K), and C are calculated and recorded in Table 2. It was found that the

Table 2. Parameters of Three Kinetic Models Calculated from Adsorption Kinetic Experiments

type of model	parameters			
	Q_e (mg/g)	K_1	R^2	X^2
pseudo-first-order	199.7	2.3×10^{-3}	0.88868	16.65
type of model	parameters			
	Q_e (mg/g)	K_2	R^2	X^2
pseudo-second-order	1512.2	6.8×10^{-4}	0.9999	0.0049
type of model	parameters			
	$K_{11}/K_{12}/K_{13}$	$C_1/C_2/C_3$	$R_1^2/R_2^2/R_3^2$	$X_1^2/X_2^2/X_3^2$
intraparticle diffusion	122.4/ 19.5/0.9	344/1194.2/ 1457.9	0.96167/ 0.99831/ 0.95327	257/0.025/ 1.28

Au(III) adsorption amount was expeditiously increased at the initial 2 h, and the capacity reached 1408 mg/g (Figure 4a). Thereafter, with the increase of the adsorption time, more and more adsorption sites were occupied by gold ions and the equilibrium was finally achieved at ~ 5 h, while the capacity reached 1478 mg/g. The initial high rate may be caused by a higher Au(III) concentration gradient and facile accessibility of Au(III) to the absorbing sites. However, the dispersability of POSS-2 in water would worsen with increasing adsorption amount of Au(III) and the Au-loaded product turned into a precipitate in the system, thus making further adsorption difficult. It is found that the adsorption kinetic process estimated by the pseudo-second-order model fits well with those measured experimentally ($R^2 = 0.9999$, $X^2 = 0.0049$), contrary to the large deviation estimated by the pseudo-first-order model (Figure 4b,c). This finding indicates that the rate-

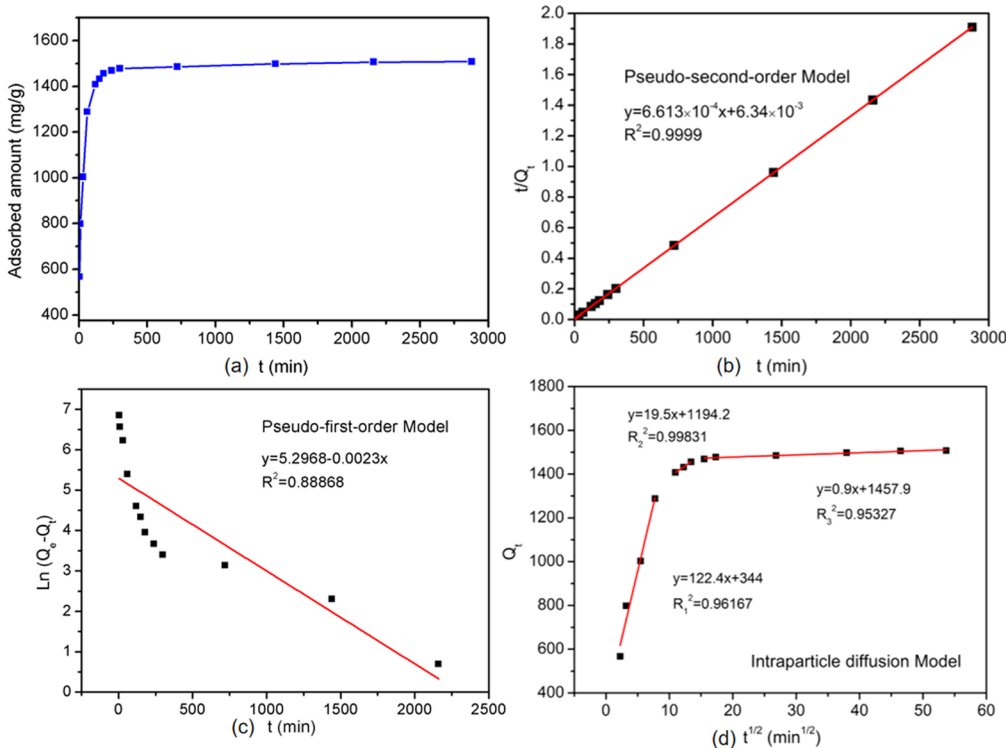


Figure 4. (a) Effect of adsorption time on the adsorbed amount of Au(III) (2000 ppm) by POSS-2 suspension in water (1 mg/mL), (b) pseudo-second-order model, (c) pseudo-first-order model, and (d) intraparticle diffusion model.

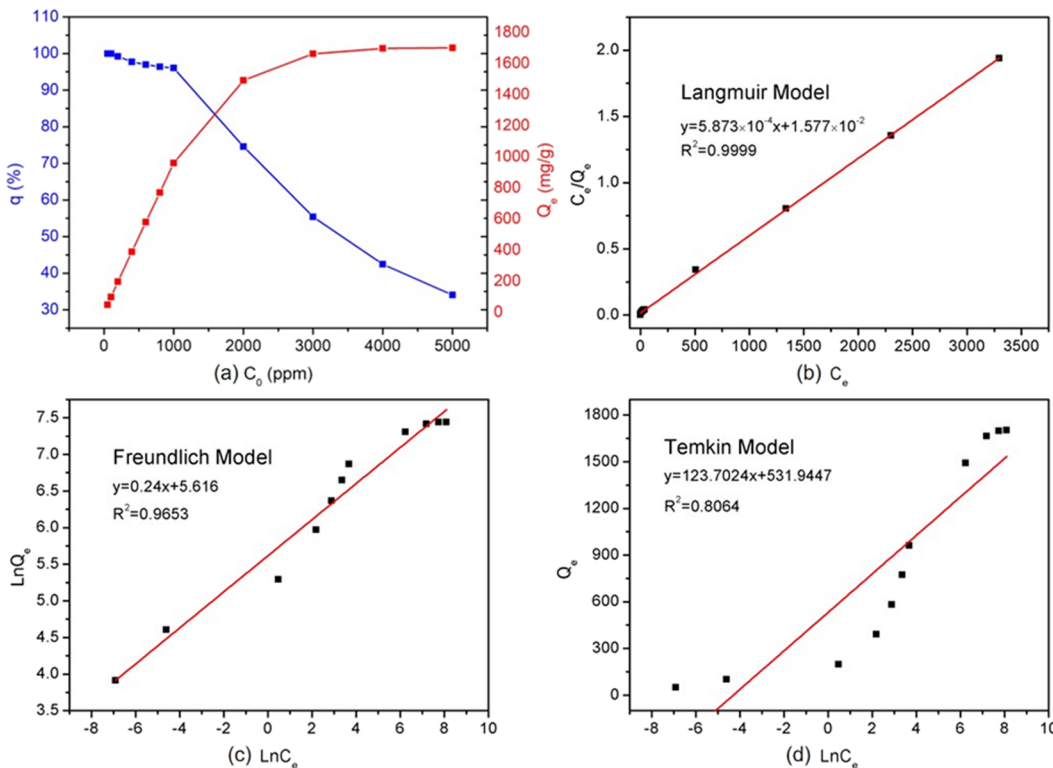


Figure 5. (a) Effect of initial Au(III) concentrations on the removal efficiency and adsorption amount of Au(III) by POSS-2 suspension in water (1 mg/mL), (b) the Langmuir model, (c) the Freundlich model, and (d) the Temkin model.

determining step is due to chemical adsorption.³³ The plot of the intraparticle diffusion model as given in Figure 4d includes three different stages, that is, external surface adsorption, internal diffusion, and adsorption process to be equilibrated.

The value of K_{i1} (122.4) is much larger than K_{i2} (19.5) and K_{i3} (0.9), indicating that the surface adsorption dominates the process.³³ After that, the gold ions diffuse in the molecular chain and the process gradually reaches the balance ($K_{i3} < 1$).

Moreover, the fitting curve did not pass the origin, thereby implying that the intraparticle diffusion model is not the dominant factor for the rate-determining step.⁴⁴ These results reveal that chemical adsorption of Au(III) by POSS-2 dominates the rate-determining step.

Adsorption Isotherm. To estimate the removal efficiency and adsorption capacity of POSS-2 toward Au(III), the equilibrium values (Q_e) were obtained by adding Au(III) aqueous solutions with the initial concentrations in the range of 50–5000 ppm. The adsorption capacity increases from 50 to 1000 ppm as the initial Au(III) concentrations increase, and the removal efficiency is as high as >90% (Figure 5a). This finding is apparently due to the driving force of the concentration gradient. Moreover, the removal efficiency can reach up to >99.99% when the initial concentration is below 100 ppm. For example, the initial Au(III) concentration at 50 ppm can be reduced to 38 ppb with a removal efficiency of 99.992%. In contrast, when the initial Au(III) concentration ranges from 1000 to 5000 ppm, the removal efficiency drops rapidly, while the adsorption growth rate slows down and the overall capacity ultimately reaches a stable value. The maximum uptake of Au(III) by POSS-2 is high and up to 1486.5 mg/g. The performance is better than most of the reported Au(III) adsorbents, such as cross-linked polyethyleneimine resins (943.5 mg/g),¹⁰ a bioadsorbent from tannin acid and dialdehyde corn starch (298.5 mg/g),⁴⁵ MoS₂ nanoflakes (1133 mg/g),¹⁷ plant tannin immobilized Fe₃O₄@SiO₂ microspheres (917.43 mg/g),⁴⁶ and metal–organic polymers (775.0 mg/g).⁴⁷ It is worthy to note that the thiourea-containing Au(III) adsorbents, including the present adsorbent POSS-2, PAF-1-thiourea (2629.87 mg/g),¹¹ and thiourea-grafted polyacrylonitrile fibers (3257.3 mg/g),⁹ possess high capacity, indicating that the thiourea group is an excellent adsorption unit for Au(III) adsorption due to its strong binding force and redox capability. The lower capacity of POSS-2 than other thiourea-containing Au(III) adsorbents could be explained by higher porosity (e.g., PAF-1-thiourea) and more abundant Au-affinity functional groups. The comparison results are summarized in Table 3.

The equilibrium adsorption isotherm data were evaluated by the Langmuir, Freundlich, and Temkin models, and the parameters are summarized in Table 4. The adsorption data can well fit the Langmuir model with a correlation coefficient (R^2) of 0.9999 and a low value of the chi-square statistic ($X^2 = 0.078$), while the other two models did not fit well with the data due to the low R^2 values of 0.9653 and 0.8064 and the high X^2 values of 0.718 and 4.07×10^4 for the Freundlich model and Temkin model, respectively. This finding indicates that the adsorption behavior of Au(III) by POSS-2 follows a monolayer adsorption.^{11,33}

Apart from the high Au(III) capacity, the adsorption selectivity is also a vital factor for Au(III) adsorption because Au(III) often coexists with other metal ions in a complex environment. The selectivity was estimated by using the POSS-2 suspension (1 mg/mL) to remove Au(III) ions (100 ppm) in the presence of various interfering metal ions, including K(I), Na(I), Ca(II), Mg(II), Al(III), Cu(II), Fe(III), Ni(II), Pb(II), Cd(II), Cr(III), and Mn(II) ions, in aqueous solutions (100 ppm). POSS-2 can completely capture Au(III) with a high removal efficiency of over 99% without a noticeable effect by other metal ions (Figure 6a). Thus, this material possessed outstanding selectivity toward Au(III) because of the better affinity between gold ions and functional groups (imidazole

Table 3. Comparison of the Maximum Capacity (Q_m) of POSS-2 with Other Au(III) Adsorbents

no.	adsorbents	Q_m (mg/g)	ref
1	PDMC-SNP	127.3	48
2	cross-linked polyethyleneimine resins	943.5	10
3	MoS ₂ nanoflakes	1133	17
4	Fe-BTC/PpPDA	934	3
5	polythioamides	597	24
6	metal–organic polymers	1317	49
7	silicon quantum dots	530	12
8	PAF-1-thiourea	2629.87	11
9	bioadsorbent from tannin acid and dialdehyde corn starch	298.5	45
10	plant tannin immobilized Fe ₃ O ₄ @SiO ₂ microspheres	917.43	46
11	metal–organic polymers	775.0	47
12	thiourea-grafted polyacrylonitrile fibers	3257.3	9
13	allylimidazole containing OSTE	48.8	21
14	MOF with mercapto-1,3,4-thiadiazole	301.5	50
15	N-(3-aminopropyl)imidazole-based poly(ionic liquid)	236.68	51
16	POSS-2	1486.5	this work

Table 4. Isotherm Parameters

type of model	parameters			
	Q_m (mg/g)	K_L (L/mg)	R^2	X^2
Langmuir	1486.5	1.02	0.9999	0.078
type of model				
Freundlich	K_F	$1/n$	R^2	X^2
	274.8	0.24	0.9653	0.718
type of model				
Temkin	K_T	b	R^2	X^2
	73.7	20.04	0.8064	4.07×10^4

thione and thioether units).¹¹ In addition, Au(III) has stronger oxidation ability than other metal ions (e.g., Cu(II), Fe(III), Ni(II), and Cd(II)),⁴⁹ and the redox process exists between the imidazole thione, thioether units, and Au(III) (see the details in the following part of *Adsorption Mechanism*).^{37,52} Higher oxidation potential of Au(III) to imidazole thione and thioether units is a vital factor leading to a desirable selective adsorption (the redox process is shown in Scheme 2). Moreover, the pH effect in the range of 1–7 on the adsorption efficiency was investigated at the initial Au(III) concentrations of 100, 1000, and 2000 ppm. It was found that the pH effect was negligible when the concentrations were 100 and 1000 ppm (Figure 6b) because the adsorption was not saturated and POSS-2 could efficiently adsorb Au(III) by coordination or redox. However, when the concentration was 2000 ppm, the removal efficiency increased from 69.4 to 75.8% with the pH ranging from 1.12 to 6.89; then the removal efficiency decreased to 73.1% when the pH increased to 7.08. The effect can be explained by the electrostatic interaction between Au(III) and POSS-2. It is known that the existence forms of Au(III) depend on the pH in aqueous solutions and the interactions between Au(III) and other species are altered.⁵⁴ Thus, the distribution of gold species in aqueous solution under different pHs was first simulated by using a chemical equilibrium software program, i.e., visual MINTEQ. The relevant parameters are listed in Table S2. As shown in Figure

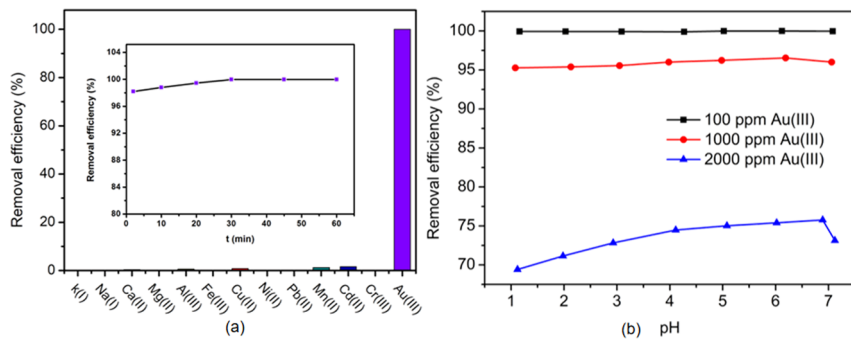
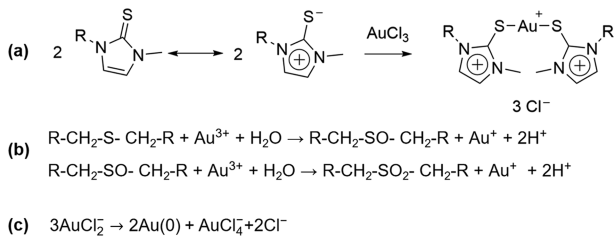


Figure 6. (a) Removal efficiency of POSS-2 toward Au(III) in the presence of various metal ions (100 ppm), and the inset is the plot of removal efficiency of Au(III) as a function of time. (b) The pH effect on the removal efficiency of Au(III) (100, 1000, and 2000 ppm) by POSS-2 (1 mg/mL) in aqueous solutions.

Scheme 2. Possible Redox Process of POSS-2 after Adsorption of Gold Ions: (a) the Imidazole Thione Groups Reduce Au(III) to Au(I), (b) the Thioether Reduces Au(III) to Au(I), and (c) the Disproportionation Reaction of Au(I) in Aqueous Solution



S6, under a low acidic condition ($\text{pH} < 3$), the main existence form of gold ions is AuCl_4^- . When the pH further increases,

the hydroxo-containing compounds, including $\text{AuCl}_3(\text{OH})^-$, $\text{AuCl}_2(\text{OH})_2^-$, and $\text{Au}(\text{OH})_3(\text{H}_2\text{O})^-$, appear. When the pH increases to 7, $\text{Au}(\text{OH})_4^-$ appears,⁵⁵ while AuCl_4^- , $\text{AuCl}_3(\text{OH})^-$, and $\text{AuCl}_2(\text{OH})_2^-$ disappear in the system. Therefore, at lower pH, Cl^- may compete with AuCl_4^- to attack the cationic imidazole ring, which is formed by the intrinsic zwitterionic resonant structure of imidazole thione. With an increment of pH, the newly formed hydroxo-containing compounds may have higher binding interactions than AuCl_4^- , thereby resulting in higher adsorption efficiency at higher pH. However, when the pH value exceeds 7, the formed $\text{Au}(\text{OH})_4^-$ might not be adsorbed by POSS-2, thus resulting in a low removal efficiency.⁵⁵ Based on these results, the pH effect on the adsorption ability is limited and generally stable compared to many adsorption processes.^{33,45,49,56} These results reveal that this material could be utilized as a stable

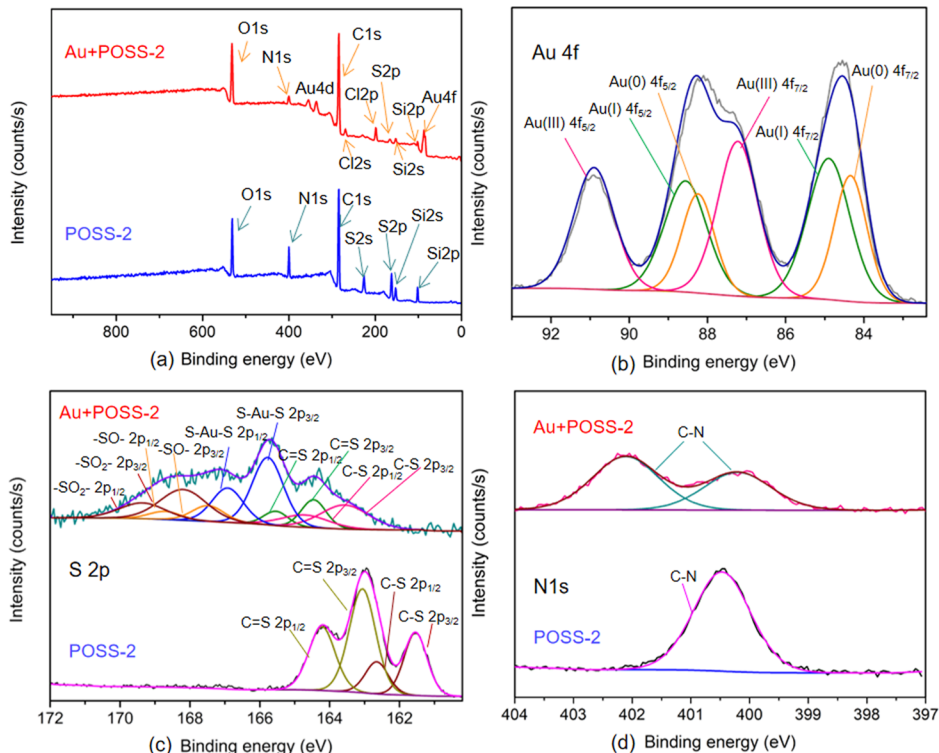


Figure 7. XPS spectra (a), high-resolution spectra of Au4f (b), high-resolution spectra of S2p (c), and high-resolution spectra of N1s (d), before and after adsorption of Au(III) by POSS-2.

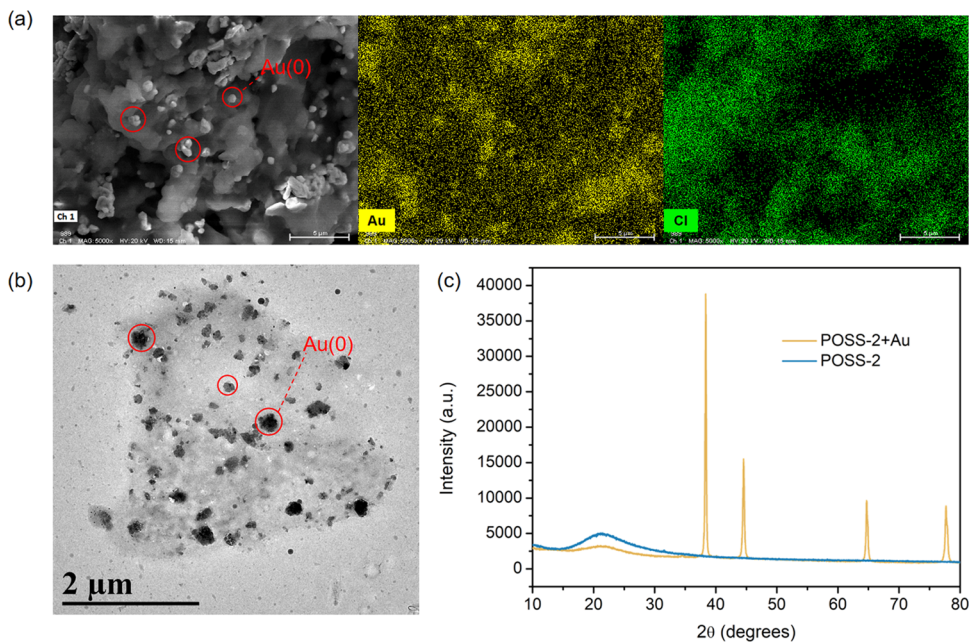


Figure 8. (a) FE-SEM image of POSS-2 after adsorbing Au(III) and elemental mappings of Au and Cl. (b) TEM image of POSS-2 after adsorbing Au(III). (c) PXRD patterns of POSS-2 before and after adsorption of Au(III).

adsorbent for selectively removing Au(III) from aqueous solutions.

Adsorption Mechanism. To deeply investigate the adsorption mechanism, XPS was used to analyze the chemical composition of POSS-2 and Au-loaded POSS-2. Prior to adsorption tests, POSS-2 contains seven primary peaks at binding energies (BEs) of 284.8, 532.0, 400.7, 232.0, 162.8, 152.8, and 101.84 eV, which refer to C1s, O1s, N1s, S2s, S2p, Si2s, and Si2p (Figure 7a), respectively. After adsorption, new Au4f ($\text{Au4f}_{7/2}$ and $\text{Au4f}_{5/2}$) peaks and one Cl2p peak appeared at BEs of ~88 and 199 eV (Figure 7a), indicating the successful Au(III) adsorption. To figure out the electronic state of gold adsorbed on POSS-2, the Au4f peak was further resolved into Au(III), Au(I), and Au(0) (Figure 7b). The fitted peaks at BEs of 84.34 and 88.24 eV are attributed to $\text{Au4f}_{7/2}$ and $\text{Au4f}_{5/2}$ from Au(0), while the peaks at BEs of 84.90 and 88.56 eV are assigned to $\text{Au4f}_{7/2}$ and $\text{Au4f}_{5/2}$ from Au(I), and the peaks at 87.22 and 90.90 eV correspond to $\text{Au4f}_{7/2}$ and $\text{Au4f}_{5/2}$ from Au(III), respectively. The calculated percentages for Au(0), Au(I), and Au(III) are 25.2, 36.6, and 38.2% respectively. The appearance of Au(0) and Au(I) verified the occurrence of a reduction reaction of Au(III) during the adsorption process. This reduction process is probably induced by the soft nucleophile-sulfur compounds and Au(III), which has been proven in thioethers and monodentate heterocyclic thiones.³⁷

Apart from the reduction mechanism, the coordination interaction between Au(III) and sulfur atoms from thione or thioether groups in POSS-2 is another important adsorption mechanism, as evidenced by the variation of the binding energy of S2p in the XPS spectra of POSS-2 before and after Au(III) adsorption. Table S3 lists the binding energies of these atoms. The S2p spectrum before adsorption is apparently determined by two chemical states in C–S and C=S groups (Figure 7c). The fitted peaks at BEs of 161.54 and 162.8 eV are assigned to S2p_{3/2} and S2p_{1/2} from S atoms in C–S groups, while the peaks at 163.03 and 164.21 eV are attributed to S2p_{3/2} and S2p_{1/2} from S atoms in C=S groups, respectively.

After adsorption, S2p peaks remarkably shift to higher binding energy values with a decreased intensity and a new peak. The binding energies of S2p_{3/2} and S2p_{1/2} in C–S groups and S2p_{3/2} and S2p_{1/2} in C=S groups increase to 163.57, 164.72, 164.39, and 165.54 eV, indicating strong coordination interactions between Au(III) and sulfur atoms from thione or thioether groups in POSS-2. In addition, three groups of new bands are also formed from 165.77 to 169.42 eV. For the BEs of 165.77 and 166.92 eV, previous reports have demonstrated that a Au(III) complex with two imidazole thione ligands underwent reductive elimination to yield a disulfide moiety along with a Au(I) species (S–Au(I)–S).^{37,39} As shown in Scheme 2a, due to the intrinsic zwitterionic resonant structure of imidazole thione, the sulfur atoms become anionic and imidazole rings become cationic by charge delocalization.³⁶ Subsequently, a Au(III) attacks two anionic sulfur atoms of the imidazole thione group, leading to the reduction of the metal center to form the S–Au(I)–S moiety.^{40,41} The higher binding energies of 167.56, 168.71, 168.27, and 169.42 eV are associated with oxidation states of thioether, in accordance with the previous reports that the thioether can be oxidized by Au(III) to sulfone or sulfoxide in aqueous solution.^{52,57} The possible process is illustrated in Scheme 2b. Based on the above two redox processes, Au(III) is reduced to Au(I), while Au(I) is unstable and can be converted into Au(0) and Au(III) by the disproportionation reaction (Scheme 2c).^{52,53} For N1s associated with C–N groups, a single peak is observed at 400.47 eV for POSS-2, while two peaks are observed at 400.05 and 402.05 eV for Au-loaded POSS-2 (Figure 7d). This finding implies that the imidazole thione–Au(I) coordination compound having the cationic imidazole ring formed and the quaternized nitrogen atoms have a higher BE of 402.05 eV.

The adsorption of Au(III) by POSS-2 can be also verified by SEM-EDS, TEM, and XRD. The Au mapping result by EDS reveals that the element gold has been adsorbed on POSS-2 (Figure 8a and Figure S7). The atomic percentages of Au and Cl elements are 6.54 and 9.37%, respectively (Figure S8),

indicating that Au(III) not only participates in the coordination with sulfur atoms but also is reduced to Au(I) and Au(0). The TEM image also clearly indicates the deposition of nanosized gold particles within the material (Figure 8b). These results confirm the coexistence of gold ions and elemental gold in Au-loaded POSS-2. The XRD spectrum further confirms the formation of Au(0) particles. Four diffraction peaks appear at $2\theta = 38.3, 44.5, 64.8$, and 77.7° (Figure 8c), corresponding with the crystal faces of (111), (200), (220), and (311) of elemental gold according to JCPDS card number 04-0784.⁵⁸ This finding indicates a reductive formation of the Au(0) particle after Au(III) adsorption by POSS-2, consistent with previous findings that the adsorption of Au(III) is typically accompanied by a reduction reaction.^{9,59}

Hence, the adsorption mechanism can be speculated as follows. Au(III) ions were adsorbed by POSS-2 via the coordination interactions with sulfur atoms from imidazole thione and thioether groups. Partial Au(III) ions subsequently underwent a reduction reaction to Au(I) by electron donors from sulfur atoms in thione and thioether groups in aqueous solution, while Au(I) was unstable in aqueous solution and could be converted into Au(0) and Au(III) by the disproportionation reaction. In other words, chelation and redox reactions simultaneously occurred during the adsorption process. In addition, under acid conditions, an electrostatic interaction between AuCl_4^- and the cationic imidazole ring also occurred as a result of the electronic delocalization of the imidazole thione upon the coordination.

As mentioned above, most of the previous materials applied in Au(III) detection and recovery commonly focus on one aspect, i.e., detection or recovery. The demand for dual-function materials with simultaneous Au(III) detection and recovery is ever-increasing from the cost and energy-saving viewpoint. Although some dual-function materials have been reported, the comprehensive property is still not satisfied as summarized in Table 5. Herein, in the present material POSS-

materials, such as silicon quantum dots (LOD: 13.67 ppb, Q_m : 530.7 mg/g),¹² thioether-functionalized covalent-organic frameworks (LOD: 0.87 μM , Q_m : 560 mg/g),¹⁴ and conjugate adsorbent (LOD: 0.11 ppb, Q_m : 203.42 mg/g).²⁷ Moreover, the insolubility but good dispersability in water of POSS-2 means that the material can efficiently detect and adsorb gold from a solid–liquid heterogeneous system, thereby facilitating the separation of the adsorbed product and reusability of this material.

Reusability of POSS-2 for Capturing Au(III). The reusability of POSS-2 for capturing Au(III) was also evaluated. Considering that the adsorption mechanism of POSS-2 for Au(III) embraces redox and chelation, a suitable desorption method should be applied for the recycling process. Herein, ascorbic acid was used to reduce the remaining chelate Au(III) and Au(I) to Au(0), and thus, the chelate sites were released. In addition, the S-containing adsorption sites of POSS-2 after the adsorption of gold ions can be restored to the oxidation state by ascorbic acid.⁹ As shown in Figure S9, the adsorption ability of Au(III) by POSS-2 decreased as the regeneration cycles increased, while the adsorption experiments were performed by applying POSS-2 (1 mg/mL) to capture Au(III) in aqueous solutions with a concentration of 500 ppm for 2 h. It is found that the adsorption ability was decreased to 88% after five recycling tests. This finding could be explained by the continual accumulation of reduced Au(0) on the surface of POSS-2 after adsorption, resulting in the hindrance of adsorption sites. This result demonstrates that POSS-2 as an efficient adsorbent for recovering Au(III) can be also recycled.

Recovery Gold from e-Waste. To demonstrate the practical usage of the present adsorbent in real-life applications, POSS-2 was used to extract gold from the discard CPU. SEM-EDS of the CPU unit surface displays uniform distributions of metal elements, mainly containing Cu, Ni, and Au (Figure 10a). The metal scraps were removed from the CPU and soaked into a leaching aqueous solution containing NBS and pyridine. The resulting blue solution contained 1029.5 ppm of Cu(II), 75.78 ppm of Ni(II), and 10.43 ppm of Au(III) as evaluated by AAS. POSS-2 was placed into this solution without any pH adjustment. It was found that only Au(III) can be selectively recovered from the solution and the removal efficiency reached up to 98.9% with an adsorbent dosage of 0.1 mg/mL after 1 h of adsorption (Figure 10b and Figure S10). Moreover, the gold can be recycled. After pyrolysis of Au-loaded POSS-2 at 1000 °C for 3 h and subsequent treatment with hydrofluoric acid for 24 h, gold was obtained with a purity of 92.8%, which was estimated by AAS and the optical microscope (Figure S11). These results demonstrate that this material can be applied as a promising adsorbent for the recovery of Au(III) from e-waste.

CONCLUSIONS

A novel imidazole thione-modified polyhedral oligomeric silsesquioxane (POSS-2) has been prepared and successfully served as a dual-function material for simultaneously selective detection and recovery of Au(III). The detection of Au(III) is rapid, highly sensitive, and selective with a very low limit of detection of 1.2 ppb and can be achieved by two modes, including observing the “turn-off” fluorescence phenomenon or “bare-eye” visualization of the color change from white to dark orange. For the recovery of Au(III), POSS-2 possesses a high and selective adsorption capacity toward Au(III) with a maximum uptake of 1486.5 mg/g. The dual-function perform-

Table 5. Comparison of LODs and Q_m s of the Materials for Simultaneous Detection and Recovery of Au(III)

no.	materials	LOD	Q_m (mg/g)	ref
1	RB-CSN	0.0152 μM	64.9 (0.33 mmol/g)	13
2	silicon quantum dots	13.67 ppb	530.7	12
3	TTB-COF	0.87 μM	560	14
4	conjugate adsorbent	0.11 ppb	203.42	27
5	protein GoS	49.24 ppb	0.0091	60
6	HSNS probe	39 nM	64	61
7	MF-CDs	31 nM	196	62
8	POSS-2	1.2 ppb (6.1 nM)	1486.5	this work

2, the introduction of abundant imidazole thione and thioether units within the POSS structure imparts it with an intriguing dual-function to simultaneously detect and extract Au(III) from aqueous solutions. As illustrated in Figure 9, POSS-2 not only can serve as a Au(III) sensor with high sensitivity and selectivity with an LOD of 1.2 ppb by fluorescence “turn-off” or color change but also can serve as an adsorbent to selectively and effectively recover Au(III) from aqueous solution with a Q_m of 1486.5 mg/g. The comprehensive property toward Au(III) is better than most dual-function

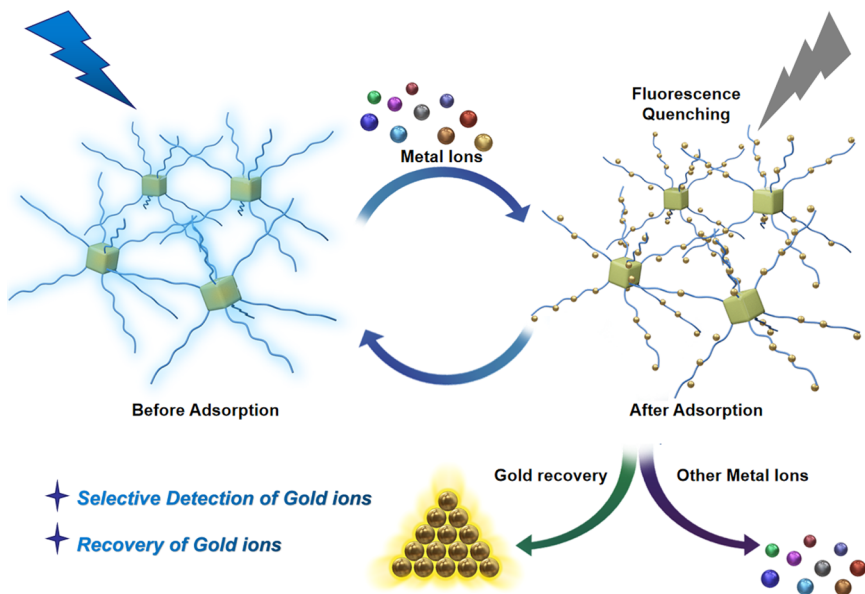


Figure 9. Schematic presentation of the detection and recovery of gold ions by POSS-2.

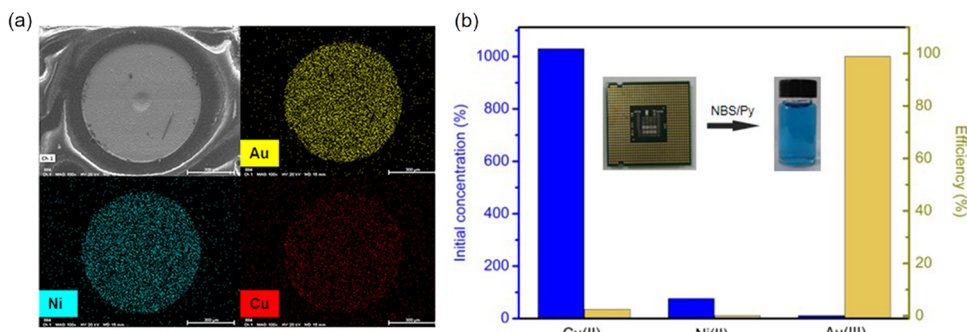


Figure 10. (a) SEM-EDS photographs of a dot on the CPU and (b) the initial concentrations of Cu(II), Ni(II), and Au(III) before adsorption and the extract efficiency of POSS-2 by extracting from the leaching solution of a discard CPU. The insets are the CPU and the leaching aqueous solution by POSS-2.

ance is better than most of the Au(III) probes and adsorbents. The mechanism investigated by XPS, SEM, and TEM indicates that the detection and adsorption were caused by the coordination and redox reaction between imidazole thione and thioether groups and Au(III). In addition, the material was also successfully applied to extract gold from e-waste. These results demonstrate that this novel imidazole thione-functionalized POSS could be promisingly utilized as a candidate for detecting and recovering Au(III) from aqueous solutions.

ASSOCIATED CONTENT

Supporting Information

The Supporting Information is available free of charge at <https://pubs.acs.org/doi/10.1021/acsami.1c01965>.

¹³C NMR and ²⁹Si NMR spectra of POSS-2 and POSS-1, TGA curve of POSS-2, detection time of Au(III), distribution model for Au aqueous species in different pHs, FE-SEM, mapping images, EDS images of POSS-2 after adsorption, regeneration of POSS-2 for capturing Au(III), removal efficiency of Au³⁺ from the CPU, optical microscope image of recycled gold, and XPS binding energies of Au, S, and N elements of POSS-2 before and after adsorption ([PDF](#))

AUTHOR INFORMATION

Corresponding Authors

Dengxu Wang — Key Laboratory of Special Functional Aggregated Materials, Ministry of Education & National Engineering Research Center for Colloidal Materials, School of Chemistry and Chemical Engineering, Shandong University, Jinan 250100, P. R. China; Shandong Key Laboratory of Advanced Organosilicon Materials and Technologies & State Key Laboratory of Fluorinated Functional Membrane Materials, Zibo 256401, P. R. China; [orcid.org/0000-0002-1139-5250](#); Email: dxwang@sdu.edu.cn

Shengyu Feng — Key Laboratory of Special Functional Aggregated Materials, Ministry of Education & National Engineering Research Center for Colloidal Materials, School of Chemistry and Chemical Engineering, Shandong University, Jinan 250100, P. R. China; [orcid.org/0000-0002-3056-2296](#); Email: fsy@sdu.edu.cn

Authors

Zixu Chen — Key Laboratory of Special Functional Aggregated Materials, Ministry of Education & National Engineering Research Center for Colloidal Materials, School of Chemistry and Chemical Engineering, Shandong University, Jinan 250100, P. R. China

and Chemical Engineering, Shandong University, Jinan 250100, P. R. China

Hongzhi Liu — Key Laboratory of Special Functional Aggregated Materials, Ministry of Education & National Engineering Research Center for Colloidal Materials, School of Chemistry and Chemical Engineering, Shandong University, Jinan 250100, P. R. China;  orcid.org/0000-0002-4821-5698

Complete contact information is available at:

<https://pubs.acs.org/10.1021/acsami.1c01965>

Notes

The authors declare no competing financial interest.

ACKNOWLEDGMENTS

This research was supported by the Shandong Provincial Natural Science Foundation (ZR2019MB028), Fluorine Silicone Materials Collaborative Fund of Shandong Provincial Natural Science Foundation (ZR2020LFG011), National Natural Science Foundation of China (21774070), Fund for Shandong Province Major Scientific and Technological Innovation Projects (2017CXGC1112), and Young Scholars Program of Shandong University.

REFERENCES

- (1) Syed, S. Recovery of Gold from Secondary Sources—A Review. *Hydrometallurgy* **2012**, *115–116*, 30–51.
- (2) Ramanan, V.; Siddaiah, B.; Raji, K.; Ramamurthy, P. Green Synthesis of Multifunctionalized, Nitrogen-Doped, Highly Fluorescent Carbon Dots from Waste Expanded Polystyrene and Its Application in the Fluorimetric Detection of Au³⁺ Ions in Aqueous Media. *ACS Sustainable Chem. Eng.* **2018**, *6*, 1627–1638.
- (3) Sun, D. T.; Gasilova, N.; Yang, S.; Oveisi, E.; Queen, W. L. Rapid, Selective Extraction of Trace Amounts of Gold from Complex Water Mixtures with a Metal-Organic Framework (MOF)/Polymer Composite. *J. Am. Chem. Soc.* **2018**, *140*, 16697–16703.
- (4) Singha, S.; Kim, D.; Seo, H.; Cho, S. W.; Ahn, K. H. Fluorescence Sensing Systems for Gold and Silver Species. *Chem. Soc. Rev.* **2015**, *44*, 4367–4399.
- (5) Park, S.-H.; Kwon, N.; Lee, J.-H.; Yoon, J.; Shin, I. Synthetic Ratiometric Fluorescent Probes for Detection of Ions. *Chem. Soc. Rev.* **2020**, *49*, 143–179.
- (6) Wang, Y.; Liu, Y.; Miao, J.; Ren, M.; Guo, W.; Lv, X. Novel Bodipy-Based Fluorescent Probe for Au³⁺ Ions with High Selectivity and Its Application to Bioimaging. *Sens. Actuators, B* **2016**, *226*, 364–369.
- (7) Li, Z.; Xu, Y.; Fu, J.; Zhu, H.; Qian, Y. Monitoring of Au(III) Species in Plants Using a Selective Fluorescent Probe. *Chem. Commun.* **2018**, *54*, 888–891.
- (8) Mackenzie, H. K.; Rawe, B. W.; Samedov, K.; Walsgrove, H. T. G.; Uva, A.; Han, Z.; Gates, D. P. A Smart Phosphine-Diyne Polymer Displays "Turn-On" Emission with a High Selectivity for Gold(I/III) Ions. *J. Am. Chem. Soc.* **2020**, *142*, 10319–10324.
- (9) Liu, J.; Jin, C.; Wang, C. Hyperbranched Thiourea-Grafted Electrospun Polyacrylonitrile Fibers for Efficient and Selective Gold Recovery. *J. Colloid Interface Sci.* **2020**, *561*, 449–458.
- (10) Liu, F.; Zhou, L.; Wang, W.; Yu, G.; Deng, S. Adsorptive Recovery of Au(III) from Aqueous Solution using Crosslinked Polyethyleneimine Resins. *Chemosphere* **2020**, *241*, 125122.
- (11) Ma, T.; Zhao, R.; Li, Z.; Jing, X.; Faheem, M.; Song, J.; Tian, Y.; Lv, X.; Shu, Q.; Zhu, G. Efficient Gold Recovery from E-Waste via a Chelate-Containing Porous Aromatic Framework. *ACS Appl. Mater. Interfaces* **2020**, *12*, 30474–30482.
- (12) Li, L.-S.; Xu, L. Highly Fluorescent Silicon Quantum Dots Decorated Silica Microspheres for Selective Detection and Removal of Au³⁺ and Subsequent Catalytic Application. *J. Ind. Eng. Chem.* **2020**, *84*, 375–383.
- (13) Liu, J.; Liu, W.; Xu, M.; Wang, B.; Zhou, Z.; Wang, L. Sensitive Detection of Au(III) Using Regenerative Rhodamine B-Functionalized Chitosan Nanoparticles. *Sens. Actuators, B* **2016**, *233*, 361–368.
- (14) Zhou, Z.; Zhong, W.; Cui, K.; Zhuang, Z.; Li, L.; Li, L.; Bi, J.; Yu, Y. A Covalent Organic Framework Bearing Thioether Pendant Arms for Selective Detection and Recovery of Au from Ultra-low Concentration Aqueous Solution. *Chem. Commun.* **2018**, *54*, 9977–9980.
- (15) Liu, F.; Zhou, Z.; Li, G. Persimmon Tannin Functionalized Polyacrylonitrile Fiber for Highly Efficient and Selective Recovery of Au(III) from Aqueous Solution. *Chemosphere* **2021**, *264*, 128469.
- (16) Zhao, M.; Huang, Z.; Wang, S.; Zhang, L. Ultrahigh Efficient and Selective Adsorption of Au(III) from Water by Novel Chitosan-Coated MoS₂ Biosorbents: Performance and Mechanisms. *Chem. Eng. J.* **2020**, *401*, 126006.
- (17) Feng, B.; Yao, C.; Chen, S.; Luo, R.; Liu, S.; Tong, S. Highly Efficient and Selective Recovery of Au(III) from a Complex System by Molybdenum Disulfide Nanoflakes. *Chem. Eng. J.* **2018**, *350*, 692–702.
- (18) Zhou, H.; Ye, Q.; Xu, J. Polyhedral Oligomeric Silsesquioxane-Based Hybrid Materials and Their Applications. *Mater. Chem. Front.* **2017**, *1*, 212–230.
- (19) Chardin, C.; Rouden, J.; Livi, S.; Baudoux, J. Dimethyldioxirane (DMDO) as a Valuable Oxidant for the Synthesis of Polyfunctional Aromatic Imidazolium Monomers Bearing Epoxides. *Green Chem.* **2017**, *19*, 5054–5059.
- (20) Li, L.; Liu, H. Rapid Preparation of Silsesquioxane-Based Ionic Liquids. *Chem. – Eur. J.* **2016**, *22*, 4713–4716.
- (21) Oya, A. U.; Esra, D. A.; Emrah, Ç. Allylimidazole Containing OSTE Based Photocured Materials for Selective and Efficient Removal of Gold from Aqueous Media. *Microchem. J.* **2019**, *146*, 887–1003.
- (22) Robati, D.; Mirza, B.; Rajabi, M.; Moradi, O.; Tyagi, I.; Agarwal, S.; Gupta, V. K. Removal of Hazardous Dyes-BR 12 and Methyl Orange using Graphene Oxide as an Adsorbent from Aqueous Phase. *Chem. Eng. J.* **2016**, *284*, 687–697.
- (23) Lin, S.; Kumar Reddy, D. H.; Bediako, J. K.; Song, M.-H.; Wei, W.; Kim, J.-A.; Yun, Y.-S. Effective Adsorption of Pd(II), Pt(IV) and Au(III) by Zr(IV)-Based Metal–Organic Frameworks from Strongly Acidic Solutions. *J. Mater. Chem. A* **2017**, *5*, 13557–13564.
- (24) Cao, W.; Dai, F.; Hu, R.; Tang, B. Z. Economic Sulfur Conversion to Functional Polythioamides through Catalyst-Free Multicomponent Polymerizations of Sulfur, Acids, and Amines. *J. Am. Chem. Soc.* **2020**, *142*, 978–986.
- (25) Dolai, B.; Nayim, S.; Hossain, M.; Pahari, P.; Kumar Atta, A. A Triazole Linked C-Glycosyl Pyrene Fluorescent Sensor for Selective Detection of Au³⁺ in Aqueous Solution and Its Application in Bioimaging. *Sens. Actuators, B* **2019**, *279*, 476–482.
- (26) Park, S. Y.; Choi, M. G.; Lim, D. S.; Chang, S.-K. Fluorometric Determination of Au³⁺ via Hydrolysis of Thiocarbonate with Bromide as a Masking Agent. *Dyes Pigm.* **2019**, *164*, 14–19.
- (27) Awual, M. R.; Ismael, M. Efficient Gold(III) Detection, Separation and Recovery from Urban Mining Waste Using a Facial Conjugate Adsorbent. *Sens. Actuators, B* **2014**, *196*, 457–466.
- (28) Kundu, A.; Layek, R. K.; Kuila, A.; Nandi, A. K. Highly Fluorescent Graphene Oxide-Poly(Vinyl Alcohol) Hybrid: An Effective Material for Specific Au³⁺ Ion Sensors. *ACS Appl. Mater. Interfaces* **2012**, *4*, 5576–5582.
- (29) Yang, K.; Pan, L.; Gong, L.; Liu, Q.; Li, Z.; Wu, L.; He, Y. Colorimetric and Visual Determination of Au(III) Ions Using PEGylated Gold Nanoparticles. *Microchim. Acta* **2018**, *185*, 95.
- (30) Yim, D.; Yoon, H.; Lee, C. H.; Jang, W. D. Light-Driven Au(III)-Promoted Cleavage of Triazole-Bearing Amine Derivatives and Its Application in The Detection of Ionic Gold. *Chem. Commun.* **2014**, *50*, 12352–12355.

- (31) Karakuş, E.; Üçüncü, M.; Emrullahoglu, M. A Rhodamine/BODIPY-Based Fluorescent Probe for The Differential Detection of Hg(II) and Au(III). *Chem. Commun.* **2014**, *50*, 1119–1121.
- (32) Yang, Y.; Yin, C.; Huo, F.; Chao, J. A Selective Fluorescent Probe for Detection of Gold(III) Ions and Its Application to Bioimaging. *RSC Adv.* **2013**, *3*, 9637–9640.
- (33) Chen, X.; Xiang, Y.; Xu, L.; Liu, G. Recovery and Reduction of Au(III) from Mixed Metal Solution by Thiourea-Resorcinol-Formaldehyde Microspheres. *J. Hazard. Mater.* **2020**, *397*, 122812.
- (34) Mongin, C.; Pianet, I.; Jonusauskas, G.; Bassani, D. M.; Bibal, B. Supramolecular Photocatalyst for the Reduction of Au(III) to Au(I) and High-Turnover Generation of Gold Nanocrystals. *ACS Catal.* **2014**, *5*, 380–387.
- (35) Cao, Z.; Bassani, D. M.; Bibal, B. Photoreduction of Thioether Gold(III) Complexes: Mechanistic Insight and Homogeneous Catalysis. *Chem* **2018**, *24*, 18779–18787.
- (36) Moraes, L. C.; Lacroix, B.; Figueiredo, R. C.; Lara, P.; Rojo, J.; Conejero, S. Stabilisation of Gold Nanoparticles by N-heterocyclic Thiones. *Dalton Trans.* **2017**, *46*, 8367–8371.
- (37) Jääskeläinen, S.; Koskinen, L.; Kultamaa, M.; Haukka, M.; Hirva, P. Persistence of Oxidation State III of Gold in Thione Coordination. *Solid State Sci.* **2017**, *67*, 37–45.
- (38) Lynch, W. E.; Padgett, C. W.; Quillian, B.; Haddock, J. A Square-planar Hydrated Cationic Tetrakis(methimazole) Gold(III) Complex. *Acta Cryst.* **2015**, *71*, 298–300.
- (39) Jia, W. G.; Dai, Y. C.; Zhang, H. N.; Lu, X.; Sheng, E. H. Synthesis and Characterization of Gold Complexes with Pyridine-Based SNS Ligands and as Homogeneous Catalysts for Reduction of 4-Nitrophenol. *RSC Adv.* **2015**, *5*, 29491–29496.
- (40) Fettouhi, M.; Wazeer, M. I. M.; Isab, A. A. Crystal Structure of Dibromo-Bis(1,3-Imidazolidine-2-Thione-S) Zinc(II), $ZnBr_2(C_3H_6N_2S)_2$. *Z. Kristallogr. - New Cryst. Struct.* **2006**, *221*, 221–222.
- (41) Hussain, M. S.; Isab, A. A. Bis(N-Propyl-1,3-Imidazolidine-2-Thione)Gold(I) Chloride: Crystal and Molecular Structure. *Transition Met. Chem.* **1985**, *10*, 178–181.
- (42) Liao, J.; Cheng, Z.; Zhou, L. Nitrogen-Doping Enhanced Fluorescent Carbon Dots: Green Synthesis and Their Applications for Bioimaging and Label-Free Detection of Au^{3+} Ions. *ACS Sustainable Chem. Eng.* **2016**, *4*, 3053–3061.
- (43) Zhou, L.; He, B.; Huang, J.; Cheng, Z.; Xu, X.; Wei, C. Multihydroxy Dendritic Upconversion Nanoparticles with Enhanced Water Dispersibility and Surface Functionality for Bioimaging. *ACS Appl. Mater. Interfaces* **2014**, *6*, 7719–7727.
- (44) Wang, J.; Li, Z.; Hu, N.; Liu, L.; Huang, C.; Yang, Q.; Wang, Y.; Suo, Y.; Wang, T.; Wang, J. From Lamellar to Hierarchical: Overcoming the Diffusion Barriers of Sulfide-Intercalated Layered Double Hydroxides for Highly Efficient Water Treatment. *J. Mater. Chem. A* **2017**, *5*, 22506–22511.
- (45) Liu, F.; Peng, G.; Li, T.; Yu, G.; Deng, S. Au(III) Adsorption and Reduction to Gold Particles on Cost-effective Tannin Acid Immobilized Dialdehyde Corn Starch. *Chem. Eng. J.* **2019**, *370*, 228–236.
- (46) Fan, R.; Min, H.; Hong, X.; Yi, Q.; Liu, W.; Zhang, Q.; Luo, Z. Plant Tannin Immobilized $Fe_3O_4@SiO_2$ Microspheres: a Novel and Green Magnetic Bio-sorbent with Superior Adsorption Capacities for Gold and Palladium. *J. Hazard. Mater.* **2019**, *364*, 780–790.
- (47) Zhou, S.; Mo, X.; Zhu, W.; Xu, W.; Tang, K.; Lei, Y. Selective Adsorption of Au(III) with Ultra-fast Kinetics by a New Metal-Organic Polymer. *J. Mol. Liq.* **2020**, *319*, 114125.
- (48) Fu, L.; Zhang, L.; Wang, S.; Zhang, B.; Peng, J. Selective Recovery of Au(III) from Aqueous Solutions by Nanosilica Grafted with Cationic Polymer: Kinetics and Isotherm. *J. Taiwan Inst. Chem. Eng.* **2017**, *80*, 342–348.
- (49) Xu, W.; Mo, X.; Zhou, S.; Zhang, P.; Xiong, B.; Liu, Y.; Huang, Y.; Li, H.; Tang, K. Highly Efficient and Selective Recovery of Au(III) by a New Metal-Organic Polymer. *J. Hazard. Mater.* **2019**, *380*, 124221.
- (50) Wang, C.; Lin, G.; Zhao, J.; Wang, S.; Zhang, L. Enhancing Au(III) Adsorption Capacity and Selectivity via Engineering MOF with Mercapto-1,3,4-Thiadiazole. *Chem. Eng. J.* **2020**, *388*, 124221.
- (51) Gui, W.; Shi, Y.; Wei, J.; Zhang, Z.; Li, P.; Xu, X.; Cui, Y.; Yang, Y. Synthesis of N-(3-Aminopropyl)Imidazole-Based Poly(Ionic Liquid) as an Adsorbent for the Selective Recovery of Au(III) Ions from Aqueous Solutions. *New J. Chem.* **2020**, *44*, 20387–20395.
- (52) Qu, R.; Sun, C.; Ji, C.; Xu, Q.; Wang, C.; Cheng, G. The Sorption Mechanism of Au(III) on Sulfur-containing Chelating Resin Poly[4-Vinylbenzyl (2-Hydroxyethyl) Sulfide]. *Eur. Polym. J.* **2006**, *42*, 254–258.
- (53) Gammons, C. H.; Yu, Y.; Williams-Jones, A. E. The Disproportionation of Gold(I) Chloride Complexes at 25 to 200°C. *Geochim. Cosmochim. Acta* **1997**, *61*, 1971–1983.
- (54) Cohen, D. R.; Waite, T. D. Interaction of Aqueous Au Species with Goethite, Smectite and Kaolinite. *Geochem.: Explor., Environ., Anal.* **2004**, *4*, 279–287.
- (55) Pilśniak-Rabiega, M.; Trochimczuk, A. W. Selective Recovery of Gold on Functionalized Resins. *Hydrometallurgy* **2014**, *146*, 111–118.
- (56) Xiong, C.; Li, Y.; Wang, S.; Zhou, Y. Functionalization of Nanosilica via Guanidinium Ionic Liquid for the Recovery of Gold Ions from Aqueous Solutions. *J. Mol. Liq.* **2018**, *256*, 183–190.
- (57) Ericson, A.; Elding, L. I.; Elmroth, S. K. C. Kinetics and Mechanism of Reduction of Gold(III) Complexes by Dimethyl Sulfide. *J. Chem. Soc., Dalton Trans.* **1997**, *7*, 1159–1164.
- (58) Wang, J.; Li, J.; Wei, J. Adsorption Characteristics of Noble Metal Ions onto Modified Straw Bearing Amine and Thiol Groups. *J. Mater. Chem. A* **2015**, *3*, 18163–18170.
- (59) Bui, T. H.; Lee, W.; Jeon, S. B.; Kim, K. W.; Lee, Y. Enhanced Gold(III) Adsorption Using Glutaraldehyde-Crosslinked Chitosan Beads: Effect of Crosslinking Degree on Adsorption Selectivity, Capacity, and Mechanism. *Sep. Purif. Technol.* **2020**, *248*, 116989.
- (60) Wei, W.; Zhu, T.; Wang, Y.; Yang, H.; Hao, Z.; Chen, P. R.; Zhao, J. Engineering a Gold-Specific Regulon for Cell-Based Visual Detection and Recovery of Gold. *Chem. Sci.* **2012**, *3*, 1780–1784.
- (61) Elshehy, E. A.; El-Safaty, S. A.; Shenashen, M. A.; Khairy, M. Design and Evaluation of Optical Mesocaptor for the Detection/Recovery of Au(III) from an Urban Mine. *Sens. Actuators, B* **2014**, *203*, 363–374.
- (62) Qin, S.; Yu, X.; Xu, L. Amplified Fluorescence Detection and Adsorption of Au^{3+} by the Fluorescent Melamine Formaldehyde Microspheres Incorporated with N and S Co-doped Carbon Dots. *J. Hazard. Mater.* **2021**, *405*, 123978.